

C3.3: Direct Numerical Simulation of the Taylor-Green Vortex at $Re = 1600$

A. Mastellone, F. Capuano, S. Di Benedetto and L. Cutrone

Centro Italiano Ricerche Aerospaziali (CIRA), Propulsion Unit

1 Code description

SPARK-LES is a Large-Eddy Simulation (LES) code currently under development at CIRA in the framework of the HYPROB Program, funded by the Italian Ministry of Research [1]. In a timeframe of four years, the code shall be able to 1) provide an advanced analysis tool for design purposes, and 2) reproduce the main physical phenomena occurring within a liquid-rocket thrust chamber (e.g., turbulent mixing, high-pressure combustion, acoustic instabilities) with high-fidelity numerical methods and state-of-the-art modelling. An overview of the current status is reported in [2].

SPARK-LES solves the fully compressible Navier-Stokes equations discretized on multi-block, structured grids according to the Finite-Volume (FV) method. Explicit second- and fourth-order as well as compact fourth- and sixth-order cartesian-like operators are available for reconstruction of convective and diffusive fluxes [3]. The general interpolation operator can be expressed, for a generic variable ϕ , as

$$\alpha\tilde{\phi}_{i-3/2} + \tilde{\phi}_{i-1/2} + \alpha\tilde{\phi}_{i+1/2} = \sum_{l=1}^L \gamma_l (\bar{\phi}_{i-l} + \bar{\phi}_{i+l-1}), \quad (1)$$

where $\tilde{\phi}$ and $\bar{\phi}$ are the face- and cell-averaged values of ϕ , respectively. Two methods are available to solve the tridiagonal system arising from Eq. (1) when $\alpha \neq 0$: an analytic procedure valid for periodic and uniform cases (i.e., symmetric circulant systems) [4], or a Thomas algorithm, which is generally applicable. A fully-integrated metrics approach is adopted to take into account non-uniform meshes: the coefficients of Eq. (1) are properly modified to retain the order of accuracy on stretched grids. Time-advancement is obtained by means of explicit Runge-Kutta schemes of arbitrary number of stages. SPARK-LES features an MPI parallel implementation based on multi-block partitioning of the computational domain. The MPI calls have been carefully profiled in order to minimize communication overhead. The code makes full use of Fortran 90 capabilities,

in terms of dynamic allocation, highly modular architecture and massive use of pointers for CPU efficiency and memory usage optimization.

2 Case summary

The Taylor-Green Vortex problem is defined on a triperiodic cube with sides of 2π , and the following initial conditions

$$u(x, y, z) = U_0 \sin(x/L) \cos(y/L) \cos(z/L), \quad (2a)$$

$$v(x, y, z) = -U_0 \cos(x/L) \sin(y/L) \cos(z/L), \quad (2b)$$

$$w(x, y, z) = 0, \quad (2c)$$

$$p(x, y, z) = p_0 + \frac{\rho_0 U_0^2}{16} [\cos(2x/L) + \cos(2y/L)] [\cos(2z/L) + 2]. \quad (2d)$$

As time advances, the initial distribution of vorticity is subject to vortex-stretching, thus generating small scales and eventually causing the vortices to break into turbulence. Since there is no forcing to sustain the turbulent motion, a decay is observed after transition. The incompressible problem is entirely governed by the Reynolds number $Re = \frac{\rho U_0 L}{\mu}$, equal to 1600. However, since the code solves the compressible flow equations, the other dimensional parameters have been set to yield a nearly incompressible condition, i.e. $M = 0.1$. The ideal gas equation of state is used, along with a constant Prandtl number $Pr = 0.71$. The domain has been discretized by a uniform mesh of increasing resolution, 64^3 , 128^3 and 256^3 cells. The meshes are regular cartesian grids and have been generated by an in-house tool. In this study, explicit and compact fourth-order schemes are used for both convective and diffusive fluxes. For convective fluxes, the coefficients of Eq. (1) are $\gamma_1 = 7/12$ and $\gamma_2 = -1/12$ for the explicit fourth-order scheme ($\alpha = 0$, $L = 2$) and $\gamma_1 = 3/4$ for the fourth-order compact scheme ($\alpha = 3/4$, $L = 1$). For diffusive fluxes, a formula similar to Eq. (1) is adopted, involving face-averaged gradients rather than interpolated values. For this case, the tridiagonal system is solved by the analytic procedure. Time-advancement is performed using a third-order Runge-Kutta scheme with CFL = 0.6. No artificial dissipation or filters of any type are used. The computations were run on the CIRA cluster FLAME, equipped with Intel Xeon E5-2680 @2.7 GHz processors. Results from TauBench runs gave an average time of 7.344s.

3 Results

Figure 1 shows the time-evolution of the global kinetic energy dissipation rate

$$\varepsilon = \frac{d}{dt} \frac{1}{\rho_0 \Omega} \int_{\Omega} \rho \frac{u_i u_i}{2} d\Omega \quad (3)$$

for the explicit (left) and compact (right) fourth-order schemes and for three grid resolutions. The time t^* is adimensionalized by means of L and U_0 . A

Table 1: TauBench-normalized costs to integrate until $t^* = 12$.

N	Time step [s]	Iterations	Total Work Units
64	$5.4 \cdot 10^{-5}$	6400	1130
128	$2.7 \cdot 10^{-5}$	12800	18150
256	$1.35 \cdot 10^{-5}$	25600	292280

good grid convergence is observed in both cases. The finest grid is in excellent agreement with the reference solution for both schemes. The coarse grid shows an oscillatory behavior probably due to inadequate resolution as the flow undergoes creation of smaller scales. The integrated enstrophy

$$\zeta = \frac{1}{\rho_0 \Omega} \int_{\Omega} \rho \frac{\omega_i \omega_i}{2} d\Omega \quad (4)$$

is also considered: this is as an indirect measure of the dissipation rate, through the relation $\varepsilon_{\zeta} = 2 \frac{\mu}{\rho_0} \zeta$. The time-evolution of ε_{ζ} is shown in Fig. 2. For the finest resolution, good agreement is observed also for the enstrophy-based dissipation rate, hence no significant spurious dissipation is added to the solution and turbulent scales are well resolved by the numerical scheme.

Contours of the vorticity norm on a subset of the plane $x = -\pi L$ at $t^* = 8$ are shown in Figure 3. While the lowest grid resolution captures only the concentration of vorticity, the main structures of the shear layer are described increasingly well as the mesh is refined. The result on 256^3 cells shows a satisfactory agreement with the reference solution [5]. Although the presence of spurious secondary structures is still observed, the vorticity contours are well defined for both schemes, showing adequate resolution.

The code took an average of $5 \cdot 10^{-6}$ seconds per iteration and per cell. It is worth to remark that the two schemes (explicit and compact) take roughly the same computational effort. Numerical tests show that this is true for both the procedures available to solve the tridiagonal system. The details of the simulation times are reported in Table 1.

References

- [1] Borrelli, S., de Matteis, P., Schettino, A. and Ferrigno, F., “The HYPROB Program: mastering key technologies, design and testing capabilities for space transportation rocket propulsion evolution,” *Proceedings of the 63th International Astronautical Congress*, Naples (2012), pp. 7189-7190.
- [2] Capuano, F., Mastellone, A., Di Benedetto, S., Cutrone, L. and Schettino, A., “Preliminary developments towards a high-order and efficient LES code for propulsion applications,” *Proceedings of the jointly organized WCCM XI - ECCM V - ECFD VI*, Barcelona (2014), pp. 7569–7580.

Figure 1: Kinetic energy dissipation rate as a function of the non-dimensional time t^* for fourth-order explicit (left) and compact (right) schemes.

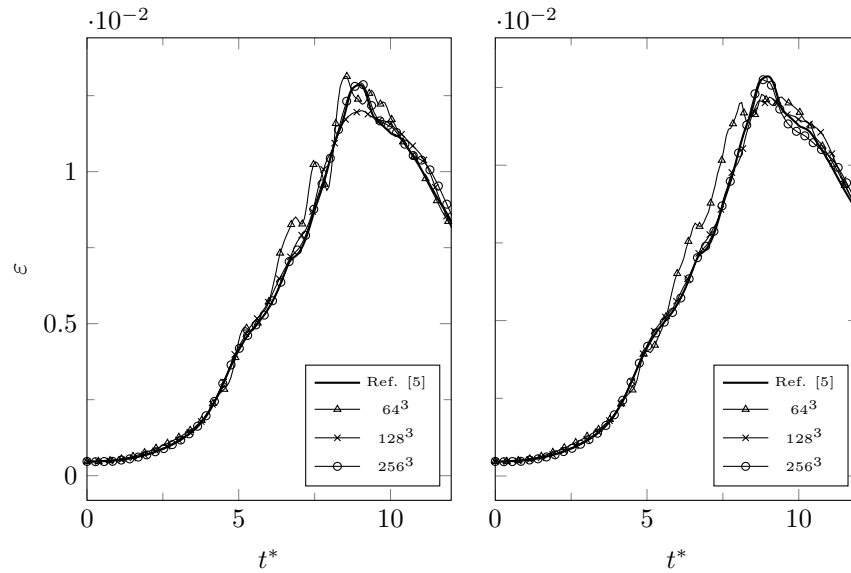


Figure 2: Enstrophy-based dissipation rate as a function of the non-dimensional time t^* for fourth-order explicit (left) and compact (right) schemes.

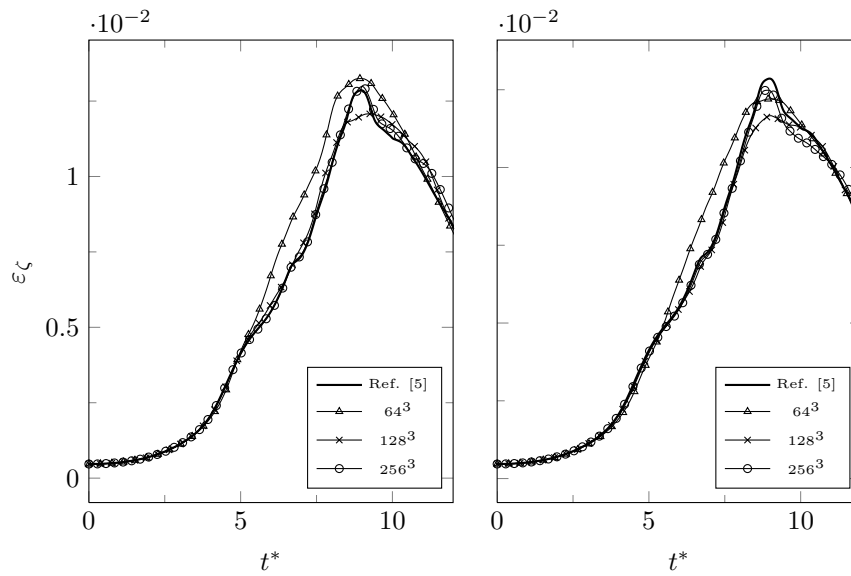
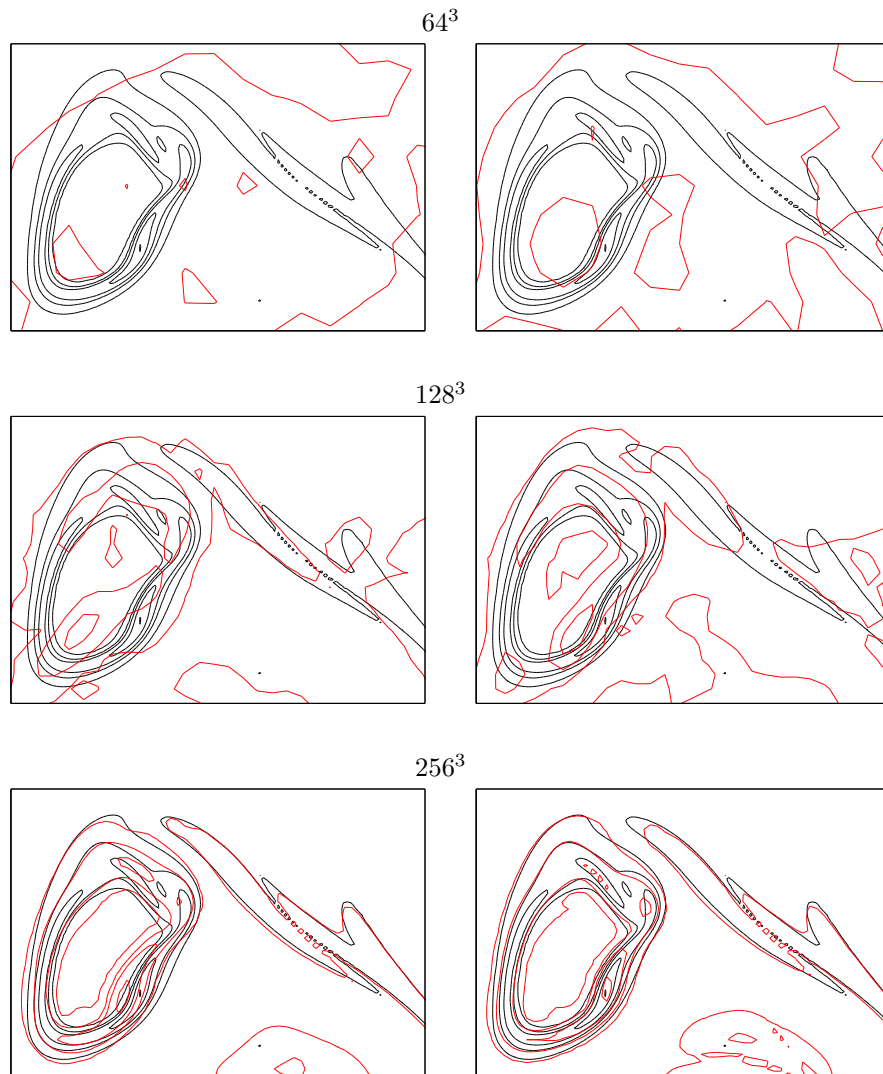


Figure 3: Contour of dimensionless vorticity norm $\frac{L}{U_0} \|\omega\| = 1, 5, 10, 20, 30$ in a subset of the periodic face $\frac{x}{L} = -\pi$ at time $t^* = 8$ on the three grids. Comparison between reference results in [5] (black) and SPARK-LES results (red) for fourth-order explicit (left) and compact (right) schemes.



- [3] Fosso, P., A., Deniau, H., Sicot, F. and Sagaut, P., “Curvilinear finite-volume schemes using high-order compact interpolation,” *J. Comput. Phys.* (2010), **229**:5090–5122.
- [4] Rojo, O., “A new method for solving symmetric circulant tridiagonal systems of linear equations,” *Computers Math. Applic.* (1990), **20**(12):61–67.
- [5] van Rees, W.M., Leonard, A., Pullin, D.I. and Koumoutsakos, P., “A comparison of vortex and pseudo-spectral methods for the simulation of periodic vortical flows at high Reynolds numbers,” *J. Comput. Phys.* (2011), **230**:2794–2805.